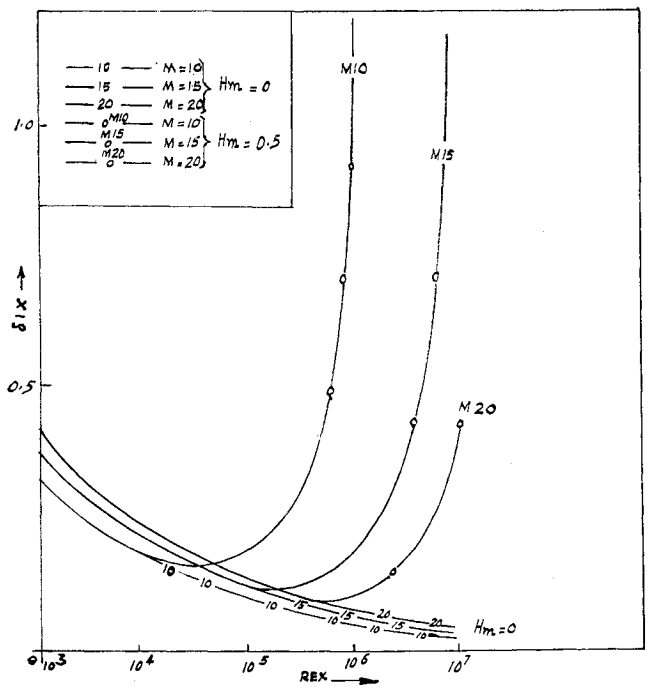

Fig. 2 Boundary-layer thickness and Reynolds number.

$P^* = 1 + \gamma M_1 d\eta/d\xi$ can be assumed to be the pressure distribution for the transition zone from strong to the weak case, so that the boundary layer thickness can be seen to proportionally vary gradually from $\xi^{3/4}$ to $\xi^{2/3}$ and then to $\xi^{1/2}$. This type of analysis gives us a complete flow picture of the magneto viscous boundary-layer interactions and this was made possible because Eq. (3) is derived to be valid for all cases unlike Ref. 1, where a similar equation of the type of Eq. 3 was valid only to the weak case, due to the approximations made therein.

The graph in Fig. 1 illustrates the behavior of δ/x with respect to Hartmann number for various local Reynolds number and the graph in Fig. 2 illustrates the behavior of δ/x with respect to local Reynolds numbers for $H_m = 0$ and $H_m = 0.5$ and for different Mach numbers. Though, the qualitative behaviour in this strong case also is the same as that of Ref. 1 yet quantitatively it is interesting to see that δ/x is being dominated by the magnetic effects for $M_1 = 10$ from $REX > 10^4$ onwards itself unlike Ref. 1, where the magnetic effects are seen appreciably only after $REX > 10^5$. The dominance of the magnetic fields after $REX > 10^4$ in comparison to Ref. 1 may be perhaps due to the reason that at these Reynolds numbers, the viscous interactions are not really strong and the dominance is obviously because, the strong viscous effects similar to Ref. 1 die out at these high Reynolds numbers. There are no magnetic effects for $REX \leq 10^4$.

In Fig. 1 and Fig. 2 the graphs of Ref. 1 are not drawn for the comparison purposes, since in the light of the present analysis the results of Ref. 1 can be taken to be valid for either a weak case or a transition case and the present results are exclusively for the strong case. Naturally δ/x for the same H_m, REX, and M_1 is higher than that of Ref. 1.

References

[1] Sastry, M. S., "Magneto Hypersonic Boundary-Layer Flow past a Plate," *AIAA Journal*, Vol. 5, No. 1, Jan. 1967, pp. 167–168.

[2] Meyer, R. C., "On Reducing Aerodynamic Heat Transfer Rates by Magnetohydro-Dynamic Techniques," *Journal of the Aerospace Sciences*, Vol. 25, 1958, pp. 561–566.

[3] Pai, S. I., "Hypersonic Viscous Flow Over an Insulated Wedge of an Angle of Attack," Rept. B.N. 42, Univ. of Maryland; also Rept. OSR-TN-54-321 Oct. 1954, Air Research and Development Command, Office of the Scientific Research.

Electron Density Measurements ahead of Shock Waves in Air

MASAYUKI OMURA* AND LEROY L. PRESLEY*
NASA Ames Research Center, Moffet Field, Calif.

THE existence of free electrons ahead of shock waves associated with high-speed bodies entering the earth's atmosphere has been ascertained from observation of both man-made entry bodies and meteors. Several laboratory studies directed toward understanding the production of precursor electrons have been conducted in diaphragm-type shock tubes.[1–3] For these studies argon was used as a working gas and the shock velocities were below 8.7 km/sec. This Note describes recent measurements of precursor electron densities in pure nitrogen and in air at shock velocities between 9.8 and 13.2 km/sec.

The experimental observations were made in a 30.48-cm-diam arc driven shock tube described in Ref. 4. The measurements were made about 13 m downstream of the diaphragm, using an 8.5 GHz microwave interferometer for the diagnostics. No significant modifications were made to the well established technique of using theoretical expressions to relate the experimentally observed phase shift of the microwave signal transmitted across the shock tube to the electron density.[5] Collimation lenses, located in both the transmitting and receiving horns were protected from the hot test gas by half-wave plates made of lucite. The interferometer has a range of sensitivity from about 10^9 to 10^{12} electrons/cm^3.

Typical electron density profiles for various shock velocities in air at an initial pressure of 0.2 torr are shown in Fig. 1. The most significant results presented in Fig. 1 are the high electron densities, in excess of 10^{10} cm^{-3} at distances greater than 5 m ahead of the higher velocity shock waves, and the large dependence of the data upon the shock wave velocity.

The high electron densities that are observed raise questions regarding the source of the electrons as well as dependency of the data upon the particular shock-tube testing technique that was used. The source of precursor electrons is widely accepted to be photoionization of the gas ahead of the shock wave. A qualitative determination of the dependency of electron production upon photoionization of the gas was obtained by placing a plastic film, which covered the entire shock-tube cross section, between the test section and the oncoming shock wave. This film, which absorbed all radiation at wavelengths shorter than 2600 Å, completely suppressed all measurable electron production in the test section. Since diffusion of electrons ahead of the shock wave is confined to very small distances, the role of radiation at wavelengths shorter than 2600 Å, i.e., ultraviolet radiation, was

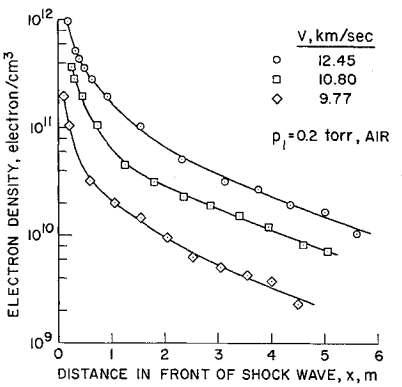

Fig. 1 Typical electron density profiles in air.

Received August 18, 1969.

* Research Scientist

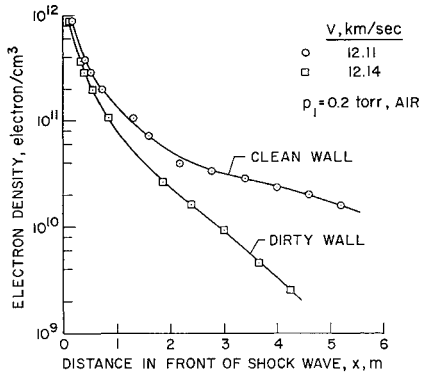

Fig. 2 Variation of electron density profiles with clean (reflecting) and dirty (nonreflecting) shock tube wall.

verified as being a major contributor to the photoionization of the gas in the test section.

At least two other features of the shock-tube test procedure could affect the results—reflection of radiation originating behind the shock wave off the shock tube walls, and leakage and outgassing affecting test gas purity. Dobbins[6] has pointed out that wall reflectivity can enhance the radiative intensity at any given location in front of the shock wave, and thus should increase the precursor electron density. In order to determine the effect of wall reflectivity, comparison was made of two shock-tube firings with differences in wall reflectivity. The first was made after the wall of the driven tube had been cleaned using a swabbing procedure. The second was made with the wall dirty, bearing a thin layer of carbonlike soot deposited from the previous firing. This layer of soot is quite black and optically absorbing over a wide spectral range, and should not alter appreciably the production of photo-electrons from the wall or the diffusion of electrons to the wall. As shown in Fig. 2, the nonreflective dirty wall considerably suppresses the production of electrons. Since the production of precursor electrons is a function of wall reflectivity, all theoretical models for the prediction of electron density ahead of a shock wave in a shock tube must include this effect. All data presented in this Note, other than that shown in Fig. 2, were taken with a clean shock-tube wall.

Several tests were made using pure nitrogen (99.99% purity) as the source gas to determine the effects of impurities in the test gas that were induced by the shock-tube testing procedure. Because of outgassing and possible leakages, it was not possible to obtain a contamination level less than 0.2% of the test gas concentration. An electron density profile ahead of a shock wave at the aforementioned minimum impurity level condition is shown in Fig. 3. When the impurity level was allowed to build up to 1% by increasing the elapsed time between charging the driven tube and firing the shock tube, nearly a five-fold increase in electron density was obtained, as shown in Fig. 3. Similar results were obtained consistently (the random scatter of all data was less than ±50%), thus demonstrating that precursor ionization in pure nitrogen is very sensitive to driven gas impurities.

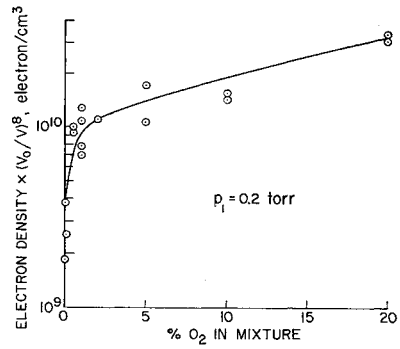

Fig. 4 Electron density at 1 m in front of shock waves for various mixtures of oxygen and nitrogen. Data adjusted to V_0 = 10 km/sec.

The most probable impurities in the nitrogen tests were water vapor and oxygen. Since it is difficult to control the concentration of water vapor, a series of firings were made wherein various mixtures of oxygen and nitrogen were used as the test gas. Although the detailed optical absorption coefficients of water vapor and oxygen are quite different, their ionization potentials are nearly identical; thus to a first approximation they should have similar response to photoionizing radiation. For these firings, the impurity concentration was maintained at the minimum level (0.2%). The electron density one meter in front of the shock wave is shown in Fig. 4 as a function of the percent oxygen in the mixture. Since shock wave velocity varied over a range of 10 to 12.5 km/sec for these data points, the electron density has been adjusted to a velocity of 10 km/sec using an eighth-power velocity dependence, which will be justified later. The magnitude of the precursor electron density is seen to be very sensitive to small amounts of oxygen up to about a 2% mixture. However, an increase in the oxygen concentration beyond 2% does not result in a proportionate increase in the electron density. For a 20% oxygen mixture, i.e., air, the difference in electron density with 0.2% and 1% unknown impurities was within the accuracy of the experiment. All data for air that are given herein are for air having an unknown impurity level of 0.2% or less.

The shock velocity dependence of the electron density one meter in front of shock waves in air is shown in Fig. 5 for three different initial pressures. The data for 0.2 and 0.4 torr appear to agree well with curves which are drawn proportional to the eighth power of shock wave velocity. However, at the lower pressure of 0.1 torr, data appear to be in better agreement with a curve that is proportional to the seventh power of shock wave velocity. The curves are drawn for comparison purposes only, and should not be given generalized interpretation.

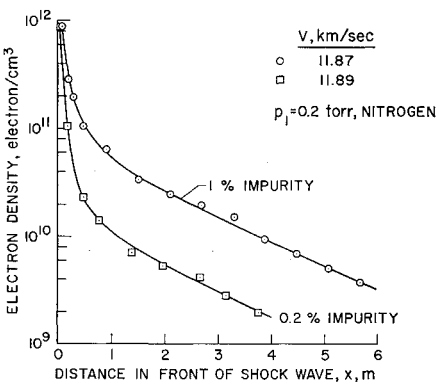

Fig. 3 Effect of impurities of unknown composition upon electron density profiles in pure nitrogen.

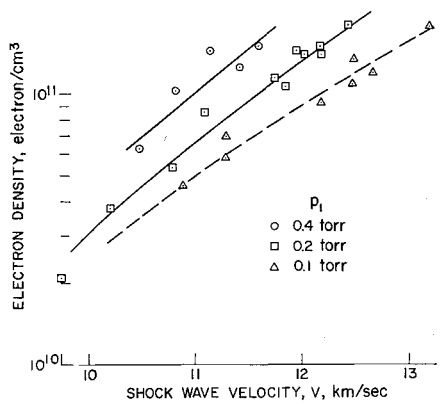

Fig. 5 Variation of electron density 1 m in front of shock with shock wave velocity.

From the data presented in this paper, several conclusions can be drawn. 1) Electron densities in excess of $10^{10}/cm^3$ are found several meters in front of shock waves travelling in air at velocities greater than 10 km/sec. 2) High reflectivity of the shock-tube wall significantly enhances the precursor electron density. 3) Driven gas impurities play a major role in the photo-ionization in pure nitrogen ahead of shock waves traveling at velocities greater than 10 km/sec. Air data, however, are much less sensitive to impurities. 4) For the shock velocity range investigated herein, $10 < V < 13$ km/sec, the precursor electron densities at initial pressures of 0.2 and 0.4 torr appear to be proportional to the eighth power of shock velocity whereas at an initial pressure of 0.1 torr the data appear to be proportional to the seventh power of velocity.

References

[1] Holmes, L. B. and Weyman, H. D., "Plasma Density Ahead of Pressure Driven Shock Waves," *Proceedings of the Fifth International Shock Tube Symposium*, Silver Spring, Md., 1965, p. 93.

[2] Lederman, S. and Wilson, D., "Microwave Resonance Cavity Measurements of Shock Produced Electron Precursors," *AIAA Journal*, Vol. 5, No. 1, Jan. 1967, pp. 70–77.

[3] Glick, H. S., "Microwave Study of Electron Precursors," *Bulletin of the American Physical Society*, Vol. 13, No. 11, Nov. 1968, p. 1518.

[4] Presley, L. L., Falkenthal, G. E., and Naff, J. T., "A 1 MJ Arc Discharge Shock Tube as a Chemical Kinetics Research Facility," *Proceedings of the Fifth Shock Tube Symposium*, Silver Spring, Md., 1965, p. 857.

[5] Heald, M. A., and Wharton, C. B., *Plasma Diagnostics with Microwaves*, Wiley, New York, 1965, pp. 192–204.

[6] Dobbins, R. A., "Photoexcitation and Photoionization of Argon ahead of a Strong Shock Wave," AIAA Paper 68-666, Los Angeles, Calif., 1968.

Investigations of Flow in Triangular Cavities

T. P. Torda* and B. R. Patel†

Illinois Institute of Technology, Chicago, Ill.

Introduction

THE experimental investigations presented are directed toward the study of flow inside triangular-shaped cavities of variable depths, induced by either steady or starting flows over the cavity mouth. Of particular interest are the time-dependent fluctuations occurring at the mouth of the cavity that may excite acoustic oscillations. Triangular shapes were chosen because they resemble baffle cavities used in liquid propellant rocket motors. These baffle cavities serve to decouple the injector from the rest of the combustion chamber where longitudinal, tangential, and radial modes of oscillations, or a combination of these, occur. The experimental setup simulated radial and tangential modes of oscillations over the cavities.

Experimental Setup and Techniques

The triangular cavity to be investigated was attached to the lower face of the test section of a specially designed wind tunnel. The direction of the airflow over the cavity is shown in Fig. 1. Two Plexiglass cavities were used, and the depths

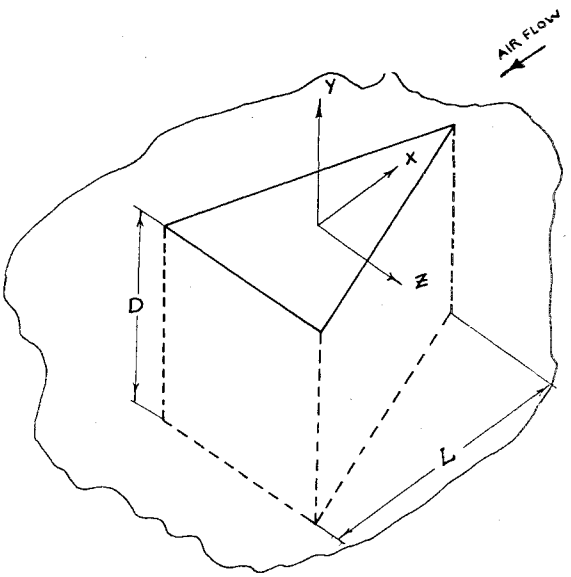

Fig. 1 Schematic diagram of the cavity.

of these cavities could be varied from 0 to 25 in. The apex angles of the triangular cavities were 60° and 30°, respectively, and each had a 10-in. base. The flow velocity was low subsonic ($0.10 < M < 0.20$), and the Reynolds number based on the height of the wind-tunnel cross section was 4.25×10^4 and larger. Hence, the flow regime was turbulent.

To understand the nature of the secondary flow induced in the cavity, it is necessary to know 1) whether the flow is steady or time-dependent, 2) the number and the size of the vortices formed in the cavity, 3) the position of these vortices, and so on. Various measurement techniques such as hot-wire anemometry, use of pressure probes for pressure measurements, flow visualization techniques, etc. may be used. Flow visualization is a fairly reliable tool in obtaining physical insight into flow regimes.

Flow visualization by injecting smoke into the air stream was tried but proved to be impractical because of rapid diffusion caused by the high level of turbulence existing at the mouth of the cavity. Hence, particles were used instead. The particles were the 3S grade of industrial "Perlites." Perlites are compounds of SiO_2, Al_2O_3, K_2O, and NaO. The bulk density of the 3S grade is 2.5 to 3 lbs/ft^3, and 92% of the particles pass through No. 30 mesh.

For steady airstreams over the cavities, the particles were injected into the airflow upstream of the test section to obtain the cavity flow pattern. In order to study the starting vortices, a layer of particles was spread at the bottom of the cavity and the airflow then was started. The particles were photographed by both high-speed (2000 frames/sec) and standard-speed (18 frames/sec) movie cameras. A frame-by-frame analysis of the resulting film gave the flow patterns shown in Figs. 2–7. To provide a better insight into the three-dimensionality of the flow, the flow patterns were photographed in both from the X direction and from the Z direction (Fig. 1).

Results and Discussion

Some of the flow patterns for the 60° apex-angle cavity as viewed from the Z direction are shown in Figs. 2–5 (the flow is from right to left). Figures 2–4 show the flow patterns in a typical shallow cavity ($L/D > 2$). The pattern shown in Fig. 2 is predominant. However, small vortices are formed intermittently near the apex as shown in Figs. 3 and 4. These small vortices are swept from the cavity and are reformed aperiodically. Figure 6 shows the same cavity, viewed from the X direction. The flow pattern clearly shows the three-dimensionality of the flow. There are two main vortices

Received May 21, 1969; revision received August 13, 1969. This research was supported by Air Force Office of Scientific Research, Office of Aerospace Research, U.S. Air Force.

* Professor, Department of Mechanical and Aerospace Engineering. Associate Fellow AIAA.

† Research Assistant, Department of Mechanical and Aerospace Engineering.